Georeferencing accuracy analysis of WorldView-02 and IKONOS images of Singapore based on RPFs

Tao Wang and Armin Gruen

Future Cities Laboratory, Singapore ETH Centre, Singapore
tawang@ethz.ch, agruen@geod.baug.ethz.ch

1 CREATE Way, #06-01 CREATE Tower, Singapore 138602

KEY WORDS: Georeferencing, Accuracy analysis, Rational polynomial functions, WorldView-2, IKONOS

ABSTRACT: High resolution satellite images provide abundant information about ground objects. In order to be used in applications like 3D building modeling and fast disaster damage monitoring, highly accurate georeferencing is a prerequisite for information extraction. Due to various reasons, rigorous sensor geometry models to derive 3D ground positions for high resolution images are not always available. In this situation, the rational polynomial coefficients (RPCs) can be utilized by a rational polynomial function model (RPF Model) for georeferencing.

This paper reports the results of accuracy analysis for georeferencing high resolution stereo images in our project in Singapore. Two pairs of stereo images covering two areas of interests are used for the analysis. One pair is DigitalGlobe's WorldView-2 panchromatic images and another is GeoEye's IKONOS pan-sharpened images. Two different software packages are used for georeferencing.

The standard RPF model is applied, but the results are not accurate enough for both image pairs.Then zero-order polynomial corrected RPFs are employed with one Ground Control Point (GCP) on each stereo pair. The results are improved remarkably by this shift correction using both software packages. Also, first-order bias corrected RPFs are used with three GCPs, which are well distributed in the images. Both tools provide very good results with sub-pixel accuracies.

The results show that georeferencing accuracies of RPFs can be substantially improved by the integration of accurate GCPs and bias correction functions.

1. INTRODUCTION

High resolution satellite images (HRSI) which have been increasingly available worldwide since the last decade can provide abundant information of geometry, texture and semantics of geographical objects with advantages in frequent revisit, multi-spectral bands and high geometrical resolution. HRSI have been used for generating various value-added products including fine resolution digital elevation models, orthorectified imagery, topographic maps and 3D models of ground features (Gruen, 2000). The usability of derived products mostly depends on the georeferencing accuracy of the original imagery during the preprocessing stage. The errors in this step can be propagated into higher level geospatial products and geospatial analysis in GIS applications, and the spatial decision making process can be negatively influenced.

Traditionally rigorous image geometry models of satellite sensors which are based on collinearity equations can be used to produce accurate transformations between 3D ground positions (object space) and 2D image positions (image space). However, due to business and reasons of confidentiality, they are not always available for final users from HRSI vendors. At the same time rigorous models are often complex and not much software and expertise are around to handle them. Therefore a large number of researchers and users have been working with non-rigorous models to approximate the rigorous ones for fast or even real-time and universal transformations (Downman and Dolloff, 2000). Various approximate geometric models, such as affine models and direct linear transformation, projective models, polynomial models, grid interpolation models and rational functions models (ratios of polynomials), have been proposed based on different approaches (OGC, 2004). A universal image geometry model (or universal sensor model) has also been proposed and accepted as NIMA standard real-time model. Among all of these approximate models, rational polynomial function (RPF) models have been widely accepted and implemented

by mainstream photogrammetric software tools. The realizations need image support information (orientation data) derived from rigorous models of imaging sensors by imagery vendors, but the implementations are independent of specific rigorous models.

After some extensive empirical investigations, the accuracies of both the physical models and the RPF models have been established for the most relevant satellites (SPOT-5, IKONOS, Quickbird, ALOS/PRISM, Cartosat-1) until about 2007 (Fraser et al, 2002; Eisenbeiss et al., 2004; Poli et al., 2004; Wolff et al., 2007). Later similar results were obtained for GeoEye-1 and WorldView-1 satellite images.

In summary, the georeferencing can be done with subpixel accuracy (0.3-0.5 pi) for both planimetric and height coordinates, independent on the satellite. Physical models and RPF models lead to almost the same accuracy level, if RPF models are amended by bias correction. Here, depending on the satellite, one to three GCPs are required at least.

In this paper, we present our working experience of georeferencing two pairs of stereo satellite images, GeoEye IKONOS and DigitalGlobe WorldView-02 of Singapore. The images were collected for the purpose of generating 3D city models. The required accuracy specifications dictate a high level of georeferencing accuracy. For orientation we apply rational polynomial functions, with the coefficients delivered by the image vendors. GCPs are used to correct the RPCs with bias compensation in two different photogrammetric software packages. The resulting residuals and RMSEs with different numbers of control points are analyzed.

2. RPF MODEL PRINCIPLE

In RPFs, image positions are represented by ratios of two polynomial functions, each of which is a third order function of ground positions and has twenty terms (figure 1). Some high order polynomials can even be zero in certain situations for easy implementation. Norrmally imagery vendors generate a group of rational polynomial coefficients for images from navigation data and distribute them to final users as metadata files to facilitate georeferencing. In order to further improve the accuracy of RPFs, a bias-compensation approach is used to refine the rational functions and reduce the orbit and calibration uncertainties (Fraser and Hanley, 2005). In figure 1, r and c are normalized image pixel positions; $f_r(r, c)$ and $f_c(r, c)$ are bias-compensation functions in image coordinate space. Usually linear functions are used, up to affine transformations, which include two shift parameters, two shear parameters and two scales. Num_{Li}, Den_{Li}, Num_{Si} and Den_{Si} are coefficients. x, y, and z are normalized ground coordinates. The four $\rho_i(x, y, z)$ functions are cubic polynomial functions with twenty terms each. The normalization of image pixels and ground positions are accompanied with RPCs.

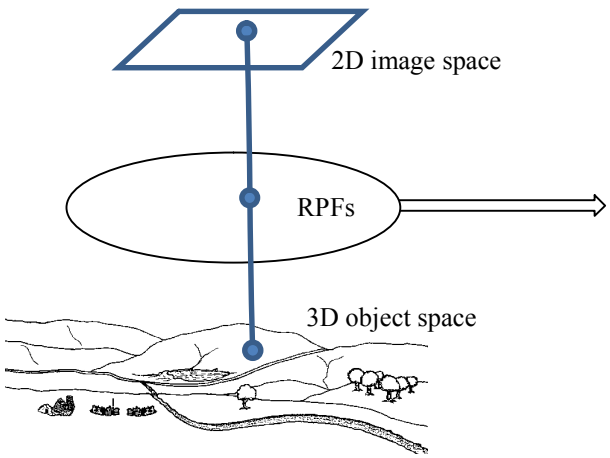

Although there are many advantages of using RPFs, disadvantages do also exist (Poli and Toutin, 2012). The solution might fail in case of highly distorted images in exceptional regions. At the same time, components of RPFs do not have corresponding physical meanings, which further causes difficulties to make an analysis of accuracies of parameters. In this way, a precise analysis of positional accuracies has to be done with ground control points (GCPs) and check points at different places.

3. STUDY SITES AND DATA

There are two study sites which are located in the northern part (Punggol) and central part (Kallang) of Singapore. The imagery for Punggol is panchromatic WorldView-02 Stereo2A. The imagery for Kallang is pan-sharpened IKONOS Geo. The basic information of the images is listed in table 1. The images have been acquired for the purpose of 3D city modeling.

Table 1. Basic information of sample images

Site	Images	Acquisition Time	Area	Cloud	Nominal GSD (Pan)
Punggol	WorldView-02	2010-12-05	13.5 km^2	0%	0.60m by 0.56m
	WorldView-02	2010-12-05	13.5 km^2	0%	0.53m by 0.50m
Kallang	IKONOS	2010-04-06	23.6 km^2	12%	0.85m by 0.85m
	IKONOS	2010-05-25	22.4 km^2	8%	1.04m by 0.92m

3.1 Punggol

Punggol is a relatively flat area and is a mixture of natural open space with minor slope, manmade landscape and high-rise buildings. The neighboring place is planned to be a new residential town by Singapore government, where infrastructures and high-rise buildings are still under construction. The DigitalGlobe WorldView-02 images are a stereo-pair covering Punggol and part of neighbouring Sekang, Singapore (figure 2). Both images were acquired on December 5, 2010. Each scene contains a panchromatic band with 0.5 meters resolution and 4 multi-spectral bands with 2 meters resolution. The two images overlap 100% and cover about 13.5 square kilometers. The panchromatic bands are resampled to 0.5 meters resolution and used for georeferencing.

WorldView-02 (Left) WorldView-02 (Right)

Figure 2. Stereo pair images of WorldView-02 of Punggol with 4 GCPs

3.2 Kallang

The Geoeye IKONOS images are a stereo-pair covering Kallang and part of neighboring regions as Geylang and Novena (figure 3). Little India is also covered. This region is covered by a combination of small and large buildings with various heights. The first image was acquired on April 06, 2010 covering about 22.4 square kilometers and the second was acquired on May 25, 2010 covering about 23.6 square kilometers. The images overlap 100%. Both images contain 4 pan-sharpened multi-spectral bands and are resampled to 1 meter resolution.

IKONOS (Left) IKONOS (Right)

Figure 3. IKONOS stereo pair of Kallang with 4 GCPs

3.3 Ground Control Points

Each stereo pair contains four ground control points (GCPs) distributed around the image corners. All GCPs are located on the clear corners of traffic marks on the roads. The GPS measurement of each GCP includes 3 minutes initializing and 5 minutes observing with at least 6 satellites. The declared horizontal accuracy is 10 mm, and the vertical accuracy 20 mm.

4. METHODS AND RESULTS

ERDAS LPS 2010 and PixelGrid v3.0 have been used with both stereo pairs for georeferencing based on rational polynomial function models. ERDAS LPS is a commercial software package for photogrammetric processing. PixelGrid v3.0 is a photogrammetric processing software package which is developed by a research group with the Chinese Academy of Surveying and Mapping (CASM) at Beijing. It has a full range of photogrammetric processing functionalities and can handle satellite and aerial imagery such as QuickBird/WorldView-I, IKONOS, SPOT1-4, SPOT-5 HRS/HRG, IRS-P5, OrbView, ALOS/PRISM and UAV images. PixelGrid is widely used in China for its typical features like high efficiency based on GPU and grid computing and high accurate DSM generation based on feature matching. PixelGrid is based on the previous version of SAT-PP (Zhang, 2005; Zhang and Gruen, 2006). CASM kindly provided us a single user license of PixelGrid v3.0 for photogrammetric image analysis in our project.

Zero order (shift transformation) and first order (affine transformation) bias corrected rational polynomial functions are implemented in both tools. When zero order polynomial corrections (shift parameters in x and y) are applied, one point is used as control point and the other 3 are used as check points for each stereo pair of images. When first order polynomial corrections (6-parameter affine transformation) are applied, three points are used as control points and the remaining one as check point. The results of the RPC model without bias corrections are also provided with ERDAS LPS. A priori standard deviation values of x, y and z for all GCPs are set to 0.03 meters.

When zero order polynomial corrected RPFs are used, the errors for the only one control point versions are zero and check points' residuals are provided in tables. When first order polynomial corrected RPFs are used, the three control point residuals are provided. Theoretically, they should be zero. The unit of ground space is in meters (m) and all results are rounded to centimeter (except for the RMSE of first order correction RPCs). The unit of image space is in pixels (pi) and rounded to 0.1 pixels. All the values are taken from triangulation reports of LPS and PixelGrid.

4.1 WorldView-02 images

4.1.1 Normal RPF transformation

In LPS, if bias compensation option is disabled, normal RPF transformation use the original RPCs only. Different combinations of control points are used to analyse the residuals. It is apparent that the residuals at both object and image spaces are far from acceptance for further applications.

Table 2. Normal RPF transformation with LPS

Check	Output Ground Residual (m)			Output Image (pi)		Control	Output Ground Residual (m)			Output Image (pi)	
	rmseX	rmseY	rmseZ	rmseX	rmseY		rmseX	rmseY	rmseZ	rmseX	rmseY
No						P_1, P_2, P_3, P_4	3.56	3.09	4.14	10.0	4.9
P_1	3.89	3.08	3.99	10.53	4.94	P_2, P_3, P_4	3.45	3.09	4.19	9.8	4.9
P_2	3.20	3.15	4.15	9.29	5.02	P_1, P_3, P_4	3.68	3.07	4.14	10.2	4.9
P_3	3.72	3.02	3.89	10.13	4.79	P_1, P_2, P_4	3.51	3.11	4.22	9.9	5.0
P_4	3.41	3.11	4.50	9.93	4.91	P_1, P_2, P_3	3.61	3.08	4.01	10.0	4.9
P_1, P_4	3.66	3.10	4.25	10.24	4.92	P_2, P_3	3.47	3.09	4.02	9.7	4.9
P_2, P_3	3.47	3.08	4.02	9.76	4.90	P_1, P_4	3.66	3.10	4.25	10.2	4.9
P_2, P_3, P_4	3.45	3.09	4.18	9.79	4.91	P_1	3.89	3.08	3.99	10.5	4.9
P_1, P_3, P_4	3.68	3.07	4.13	10.20	4.88	P_2	3.20	3.15	4.15	9.3	5.0
P_1, P_2, P_4	3.51	3.11	4.22	9.93	4.96	P_3	3.72	3.02	3.89	10.1	4.8
P_1, P_2, P_3	3.61	3.08	4.01	10.00	4.92	P_4	3.41	3.11	4.50	9.9	4.9

4.1.2 Zero order polynomial corrected RPCs

With this method, compensations are made with one control point to correct shifts of images based on RPCs. In the processing, one ground point is taken as control point and the other three points are taken as check points. The following table 2 and table 3 give the RMSEs by LPS and PixelGrid for different computational versions (GCP distributions). The residual file of PixelGrid provides only rX, rY and rZ. The RMSEs are further computed based on these values.

Table 3. Residuals based on zero order correction with one control point with LPS

		Output Ground Residual (m)			Output Image (pi)	
Control	Check	rmseX	rmseY	rmseZ	rmseX	rmseY
P_1	P_2, P_3, P_4	0.50	0.06	0.32	0.8	0.3
P_2	P_1, P_3, P_4	0.51	0.09	0.27	1.0	0.2
P_3	P_1, P_2, P_4	0.36	0.10	0.39	0.6	0.3
P_4	P_1, P_2, P_3	0.35	0.06	0.51	0.6	0.3

Table 4. Residuals based on zero order correction with one control point with PixelGrid

		Output Ground Residual (m)			Output Image (pi)	
Control	Check	rmseX	rmseY	rmseZ	rmseX	rmseY
P_1	P_2, P_3, P_4	0.18	0.29	0.74	0.1	0.0
P_2	P_1, P_3, P_4	0.13	0.39	0.57	0.1	0.0
P_3	P_1, P_2, P_4	0.09	0.21	0.58	0.1	0.0
P_4	P_1, P_2, P_3	0.10	0.22	1.06	0.1	0.0

4.1.3 First order polynomial corrected RPCs

In these versions three ground points are taken as control points. Theoretically the residuals for control points should be zero here, however some results are not, due to numerical computations or other unknown reasons.

Table 5. Residuals based on first order corrections with LPS

	Output Ground Residual (m)							Output Image (pi)	
Control	rmseX	rmseY	rmseZ	Check	rmseX	rmseY	rmseZ	rmseX	rmseY
P_2, P_3, P_4	0.0008	0.0002	0.0000	P_1	0.35	0.03	0.57	0.1	0.0
P_1, P_3, P_4	0.0004	0.0001	0.0000	P_2	0.32	0.03	0.52	0.2	0.1
P_1, P_2, P_4	0.0004	0.0001	0.0000	P_3	0.31	0.03	0.50	0.2	0.1
P_1, P_2, P_3	0.0006	0.0001	0.0000	P_4	0.29	0.03	0.46	0.2	0.1

Table 6. Residuals based on first order corrections with PixelGrid

	Output Ground Residual (m)							Output Image (pi)	
Control	rmseX	rmseY	rmseZ	Check	rmseX	rmseY	rmseZ	rmseX	rmseY
P_2, P_3, P_4	0.000	0.001	0.001	P_1	0.16	0.54	0.95	0.0	0.0
P_1, P_3, P_4	0.000	0.001	0.001	P_2	0.15	0.49	0.86	0.0	0.0
P_1, P_2, P_4	0.000	0.001	0.001	P_3	0.14	0.47	0.83	0.0	0.0
P_1, P_2, P_3	0.001	0.001	0.001	P_4	0.13	0.44	0.76	0.0	0.0

4.2 IKONOS images

The same strategies and processing pipeline as with WorldView-02 are applied to IKONOS images using both software packages. The results are listed in the corresponding tables.

4.2.1 Normal RPFs

Table 7. Normal RPF transformation with LPS

Check	Output Ground Residual (m)			Output Image (pi)		Control	Output Ground Residual (m)			Output Image (pi)	
	rmseX	rmseY	rmseZ	rmseX	rmseY		rmseX	rmseY	rmseZ	rmseX	rmseY
No						P_1, P_2, P_3, P_4	3.64	5.61	0.84	3.6	6.0
P_1	3.20	6.16	0.69	3.39	6.29	P_2, P_3, P_4	3.78	5.42	0.88	3.7	5.9
P_2	4.26	5.44	0.50	4.19	5.86	P_1, P_3, P_4	3.41	5.66	0.92	3.4	6.0
P_3	3.80	5.44	1.38	3.55	5.93	P_1, P_2, P_4	3.59	5.66	0.54	3.5	7.7
P_4	3.19	5.36	0.39	3.34	5.82	P_1, P_2, P_3	3.78	5.69	0.94	3.7	6.0
P_1, P_4	3.19	5.77	0.56	3.36	6.06	P_2, P_3	4.04	5.44	1.04	3.9	5.9
P_2, P_3	4.04	5.44	1.04	3.88	5.89	P_1, P_4	3.19	5.77	0.56	3.7	7.6
P_2, P_3, P_4	3.78	5.42	0.88	3.71	5.87	P_1	3.20	6.16	0.69	3.4	6.3
P_1, P_3, P_4	3.41	5.66	0.92	3.43	6.02	P_2	4.26	5.44	0.50	4.2	5.9
P_1, P_2, P_4	3.59	5.66	0.54	3.66	5.99	P_3	3.80	5.44	1.38	3.1	7.6
P_1, P_2, P_3	3.78	5.69	0.94	3.72	6.03	P_4	3.19	5.36	0.39	3.4	7.6

4.2.2 Zero order polynomial corrected RPCs

Table 8. Residuals based on zero order bias correction with one control point with LPS

		Output Ground Residual (m)			Output Image (pi)	
Control	Check	rmseX	rmseY	rmseZ	rmseX	rmseY
P1	P2, P3, P4	0.58	0.82	0.94	0.6	0.8
P2	P1, P3, P4	0.82	0.57	0.76	0.9	0.6
P3	P1, P2, P4	0.43	0.56	1.47	0.7	0.6
P4	P1, P2, P3	0.57	0.44	0.97	0.6	0.5

Table 9. Residuals based on zero order bias correction with one control point with PixelGrid

		Output Ground Residual (m)			Output Image (pi)	
Control	Check	rmseX	rmseY	rmseZ	rmseX	rmseY
P1	P2, P3, P4	0.64	1.06	0.98	0.1	0.2
P2	P1, P3, P4	0.42	0.81	0.84	0.1	0.1
P3	P1, P2, P4	0.36	0.58	1.59	0.1	0.2
P4	P1, P2, P3	0.37	0.68	1.24	0.1	0.2

4.2.3 First order polynomial corrected RPCs

Table 10. Residuals based on first order bias corrected RPCs with LPS

	Output Ground Residual (m)							Output Image (pi)	
Control	rmseX	rmseY	rmseZ	Check	rmseX	rmseY	rmseZ	rmseX	rmseY
P2, P3, P4	0.0001	0.0004	0.0003	P1	0.53	0.55	1.73	0.0	0.2
P1, P3, P4	0.0001	0.0005	0.0002	P2	0.49	0.50	1.57	0.1	0.3
P1, P2, P4	0.0001	0.0004	0.0002	P3	0.38	0.40	1.22	0.1	0.4
P1, P2, P3	0.0001	0.0005	0.0002	P4	0.40	0.43	1.31	0.1	0.3

Table 11. Residuals based on first order bias corrected RPCs with PixelGrid

	Output Ground Residual (m)							Output Image (pi)	
Control	rmseX	rmseY	rmseZ	Check	rmseX	rmseY	rmseZ	rmseX	rmseY
P2, P3, P4	0.0001	0.0001	0.0001	P1	0.02	0.01	0.07	0.1	0.1
P1, P3, P4	0.0001	0.0001	0.0002	P2	0.02	0.01	0.07	0.1	0.1
P1, P2, P4	0.0001	0.0001	0.0001	P3	0.01	0.00	0.07	0.1	0.1
P1, P2, P3	0.0001	0.0001	0.0002	P4	0.02	0.00	0.07	0.1	0.1

5. CONCLUSIONS

Based on two pairs of stereo images of WorldView-02 and IKONOS, georeferencing processing has been conducted with various numbers and combinations of control points and different types of RPF transformations using two different photogrammetric software packages. The normal RPF transformations without bias corrections produce errors larger than 3 to 5 meters both horizontally and vertically for both WorldView-02 and IKONOS images. With one control point provided, the bias corrections RPC with zero order polynomials are applied. The results are much better after this shift compensation. The errors for WorldView-02 images are reduced to half the GSD size by both software packages. PixelGrid performs better in planimetry and LPS slightly better vertically. With the first order polynomial correction, from the one check point (which is not enough for a thorough analysis) for each combination of control points, RPF transformations further increase the horizontal and vertical accuracies to 1 cm and 7 cm respectively in case of PixelGrid.

In summary, the results presented here are very much consistent with what has been published in the literature, also including other satellites. If done correctly, georeferencing of high resolution satellite imagery is not a critical issue any more.

ACKNOWLEDGEMENTs

We are grateful to Mr Kwoh Leong Keong of CRISP of NUS, Professor Dr. Zhang Li of Chinese Academy of Surveying and Mapping and Dr. Raju of Tropical Marine Science Institute of NUS for providing help during the data collection and software preparation phase.

REFERENCES:

1. Dowman, I., Dolloff, J., 2000. An evaluation of rational function for photogrammetric restitution. In: International Archives of Photogrammetry and Remote Sensing, Amsterdam, The Netherlands, Vol. XXXIII, Part B3, pp.252–266.
2. Eisenbeiss, H., Zhang, L, and Gruen, A., 2004. 3D precision processing of high-resolution satellite imagery. ASPRS 2005 Annual Conference, Baltimore, Maryland, USA, March 7-11, on CD-ROM.
3. Fraser, C.S., Baltsavias, E. and Gruen, A., 2002, Processing of IKONOS imagery for sub-metre 3D positioning and building extraction. ISPRS Journal of Photogrammetry and Remote Sensing, 56(3), pp. 177-194.
4. Fraser, C.S., Hanley, H. B., 2005. Bias-compensated RPCs for sensor orientation of high-resolution satellite imagery. Photogrammetric Engineering & Remote Sensing 71(8), pp. 909 – 915.
5. Gruen, A., 2000. Potential and limitations of high resolution satellite imagery. 21st Asian Conference on Remote Sensing, Taipei, Taiwan.

6. OGC (Open Geospatial Consortium Inc.), 2004. Some image geometry models. http://portal.opengeospatial.org/files/?artifact_id=7257. (Accessed on 25/08/2012).
7. Poli, D., Zhang, L., and Gruen, A., 2004. SPOT-5/HRS stereo images orientation and automated DSM generation. XXth ISPRS Congress, Istanbul, Turkey, International Archives of Photogrammetry, Remote Sensing and Spatial Information Sciences, 35(1), pp. 421-432.
8. Poli, D., Toutin T., 2012. Review of developments in geometric modelling for high resolution satellite pushbroom sensors. The Photogrammetric Record, 27(137), pp. 58–73.
9. Wolff, K., Kocaman, S., and Gruen, A., 2007. Calibration and validation of early ALOS/PRISM images. The Journal of the Japan Society of Photogrammetry and Remote Sensing, 46(1), pp. 24-38.
10. Zhang L., 2005. Automatic Digital Surface Model (DSM) Generation from Linear Array Images. PhD Dissertation, Mitteilungen Nr 88, Institute of Geodesy and Photogrammetry, ETH Zurich.
11. Zhang, L., Grün, A., 2006. Multi-image matching for DSM generation from IKONOS imagery. ISPRS Journal of Photogrammetry and Remote Sensing 60 (3), pp. 195–211.